Isolation and characterization of a structurally unique β-hairpin venom peptide from the predatory ant Anochetus emarginatus

Axel Touchard, Andreas Brust, Fernanda Caldas Cardoso, Yanni K.-Y. Chin, Volker Herzig, Ai-Hua Jin, Alain Dejean, Paul F. Alewood, Glenn F. King, Jérôme Orivel, et al.

Biochimica et Biophysica Acta 1860 (2016) 2553–2562

Contents lists available at ScienceDirect

Biochimica et Biophysica Acta

journal homepage: www.elsevier.com/locate/bbagen

Isolation and characterization of a structurally unique β-hairpin venom peptide from the predatory ant *Anochetus emarginatus*☆

Axel Touchard [a,*], Andreas Brust [b], Fernanda Caldas Cardoso [b], Yanni K.-Y. Chin [b], Volker Herzig [b], Ai-Hua Jin [b], Alain Dejean [a,c,d], Paul F. Alewood [b], Glenn F. King [b], Jérôme Orivel [a], Pierre Escoubas [e]

[a] CNRS, UMR Ecologie des forêts de Guyane (AgroParisTech, CIRAD, CNRS, INRA, Université de Guyane, Université des Antilles), Campus Agronomique, BP 316, 97379 Kourou, France
[b] Institute for Molecular Bioscience, The University of Queensland, St Lucia, Queensland 4072, Australia
[c] CNRS, UMR 5245, Laboratoire Écologie Fonctionnelle et Environnement, 118 route de Narbonne, 31062 Toulouse, France
[d] Université de Toulouse, UPS, INP, Ecolab, Toulouse, France
[e] VenomeTech, 473 Route des Dolines, 06560 Valbonne, France

ARTICLE INFO

Article history:
Received 22 February 2016
Received in revised form 24 June 2016
Accepted 26 July 2016
Available online 28 July 2016

Keywords:
Ant venom
Anochetus
Poneritoxins
U_1-PONTX-Ae1a
Disulfide-rich peptides
Neurotoxin
L-type calcium channels

ABSTRACT

Background: Most ant venoms consist predominantly of small linear peptides, although some contain disulfide-linked peptides as minor components. However, in striking contrast to other ant species, some *Anochetus* venoms are composed primarily of disulfide-rich peptides. In this study, we investigated the venom of the ant *Anochetus emarginatus* with the aim of exploring these novel disulfide-rich peptides.
Methods: The venom peptidome was initially investigated using a combination of reversed-phase HPLC and mass spectrometry, then the amino acid sequences of the major peptides were determined using a combination of Edman degradation and *de novo* MS/MS sequencing. We focused on one of these peptides, U_1-PONTX-Ae1a (Ae1a), because of its novel sequence, which we predicted would form a novel 3D fold. Ae1a was chemically synthesized using Fmoc chemistry and its 3D structure was elucidated using NMR spectroscopy. The peptide was then tested for insecticidal activity and its effect on a range of human ion channels.
Results: Seven peptides named poneritoxins (PONTXs) were isolated and sequenced. The three-dimensional structure of synthetic Ae1a revealed a novel, compact scaffold in which a C-terminal β-hairpin is connected to the N-terminal region *via* two disulfide bonds. Synthetic Ae1a reversibly paralyzed blowflies and inhibited human L-type voltage-gated calcium channels (Ca_V1).
Conclusions: Poneritoxins from *Anochetus emarginatus* venom are a novel class of toxins that are structurally unique among animal venoms.
General significance: This study demonstrates that *Anochetus* ant venoms are a rich source of novel ion channel modulating peptides, some of which might be useful leads for the development of biopesticides.

1. Introduction

Venomous animals employ complex biochemical cocktails of small molecules, peptides and proteins for the dual purpose of prey capture and defense against predators [1]. Arthropod venoms generally comprise a heterogenous mixture of proteins, peptides, salts, biogenic amines and small molecules such as alkaloids and acylpolyamines [2]. Significantly, small disulfide-rich peptides are the dominant components of most arthropod venoms that have been studied in detail to date, including those from spiders [3], scorpions [4] and centipedes [5].

The composition of the venom of other invertebrates such as insects, crustaceans and annelid worms has been less studied, with some of the first investigations performed only very recently [6–10]. Surprisingly, despite the ubiquity, abundance and diversity of ants (Hymenoptera: Formicidae), with >13,000 species described [11], their venoms remain largely unexplored. While some hymenopteran subfamilies rely on

Abbreviations: RP-HPLC, reversed phase-high performance liquid chromatography; LC, liquid chromatography; MS, mass spectrometry; ACN, acetonitrile; TFA, trifluoroacetic acid; MALDI, matrix-assisted laser desorption/ionization; TOF, time-of-flight; FA, ferulic acid; DTT, dithiothreitol; PTH, phenylthiohydantoin; DMF, dimethylformamide; DCM, dichloromethane; DIEA, diisopropylethylamine; HBTU, 2-(1H-benzotriazol-1-yl)-1,1,3,3-tetramethyluronium hexafluorophosphate; TIPS, triisopropylsilane; EDT, ethanedithiol; ESI, electrospray ionization; DMSO, dimethyl sulfoxide; nAChR, acetylcholine receptor; NMR, nuclear magnetic resonance.

☆ The protein sequence data reported in this paper will appear in the UniProt Knowledgebase under the accession numbers C0HJY4; U_1-Poneritoxin-Ae1a (U_1-PONTX-Ae1a), C0HJY5; U_1-Poneritoxin-Ae1b (U_1-PONTX-Ae1b), C0HJY6; U_1-Poneritoxin-Ae1c (U_1-PONTX-Ae1c), C0HJY7; U_1-Poneritoxin-Ae1d (U_1-PONTX-Ae1d), C0HJY8; U_1-Poneritoxin-Ae1e (U_1-PONTX-Ae1e) C0HJY9; U_1-Poneritoxin-Ae1f (U_1-PONTX-Ae1f), C0HJZ0; U_1-Poneritoxin-Ae1g (U_1-PONTX-Ae1g).

* Corresponding author at: BTST (Biochimie et Toxicologie des Substances Bioactives), Institut National Universitaire de Champollion, Place de Verdun, Albi 81012, France.
E-mail address: t.axel@hotmail.fr (A. Touchard).

http://dx.doi.org/10.1016/j.bbagen.2016.07.027
0304-4165/

small-molecule chemical defenses, such as formic acid or alkaloids, many others, including wasps, bees, bumblebees and the majority of ant species, have retained the ability to sting and those venoms appear to be peptide-rich. Preliminary investigations into the venom repertoire of stinging ants demonstrated that peptide-based ant venoms may each comprise up to 300 peptides [12,13], leading to a conservative estimate of >1,500,000 peptides in all ant venoms combined. Although such a natural peptide library has immense potential for drug and insecticide discovery, very few studies have examined the peptidome of ant venoms. Indeed, to date, a total of only 75 peptides have been sequenced from ant venoms [14,15], compared to >1000 for spiders, and there have been very few investigations of their three-dimensional structure and pharmacological activity [16–18].

The ant-venom peptides sequenced to date fall into three distinct structural classes: linear (*i.e.*, devoid of disulfide bonds); homo- and heterodimers; and inhibitor cystine knot (ICK)-like peptides. Our recent mass spectrometry-based survey of 82 stinging ant peptidomes confirmed the prevalence of small linear peptides with <35 residues and highlighted the presence of disulfide-linked peptides in most subfamilies [12]. Interestingly, this study also revealed that several venoms from the genus *Anochetus* (subfamily Ponerinae) have a peculiar composition, consisting almost entirely of monomeric peptides with one or two disulfide bonds [12]. Such disulfide-rich peptides are likely to constitute novel families of ant toxins with potentially interesting structural scaffolds and pharmacology. We therefore embarked on a study of these disulfide-rich peptidomes, with the goal of uncovering new scaffolds and linking them to useful pharmacological properties, in particular against ion channels, with a view towards development of insecticides and human therapeutics.

Anochetus are predatory ant species that subdue small invertebrate prey using their unique trapjaws (*i.e.*, forward-facing mandibles that can open to almost 180°) prior to the injection of venom. There have been no studies to date of venom from any *Anochetus* species, and consequently we initiated a detailed investigation of the venom peptidome of *A. emarginatus*. This led to the isolation and characterization of a novel family of neurotoxic disulfide-rich peptides that we named poneritoxins (PONTXs). One of these toxins (Ae1a) was shown to be insecticidal and inhibit human voltage-gated calcium channels.

2. Materials and methods

2.1. Ant collection

Live *A. emarginatus* workers were collected from both the *Nouragues* research station (N 04°05′16″, W52°40′48″) and the *Kaw* area (N 04°32′44″, W 52°08′03″) in French Guiana. Voucher specimens were deposited in the *Laboratório de Mirmecologia* collection, Cocoa Research Centre, Ilhéus, Bahia, Brazil. Worker ants were stored at −20 °C prior to dissection. Ant venom sacs were dissected and pooled in 10% v/v acetonitrile (ACN)/water. Samples were centrifuged for 5 min at 14,400 rpm, then the supernatant was collected and lyophilized prior to storage at −20 °C until further use. Fifty ant venom sacs dissected from three different colonies collected at the Nouragues station were used for investigation of the venom peptidome as well as for the isolation and sequencing of poneritoxins. Furthermore, a supplementary venom sample was obtained with 70 venom sacs from a single colony, collected at Kaw. This sample was used to check for coelution of native and synthetic poneritoxin on RP-HPLC, and for a preliminary pharmacological screening of the effect of crude venom on human ion channels.

2.2. RP-HPLC separation and peptide purification

A. emarginatus venom was fractionated by semi-micro RP-HPLC using an Xterra-C_{18} column (5 μm, 2.1 × 100 mm; Waters, USA) with a gradient comprised of solvent A (0.1% v/v trifluoroacetic acid (TFA)) and solvent B (acetonitrile (ACN)/0.1% v/v TFA). The percentage of solvent B was modified as follows: 0% for 5 min, 0–60% over 60 min, and 60–90% over 10 min at a flow rate of 0.3 $ml \cdot min^{-1}$. The eluate was monitored by UV absorbance at 215 nm using a diode-array detector. All analyses were performed on an Agilent HP 1100 system (Agilent, USA). Peptide elution was monitored in real time and fractions were collected manually for each eluting peak. Each fraction was dried and reconstituted in 50 μL of 0.1% v/v TFA/water for offline matrix-assisted laser desorption/ionization time-of-flight mass spectrometry (MALDI-TOF MS) analysis. Further peptide purification was achieved by subjecting C_{18} fractions to a second reversed-phase chromatography step on a Jupiter C_4 column (5 μm, 4.6 × 250 mm; Phenomenex, USA).

2.3. Mass spectrometry analysis

MS analyses were performed on a Voyager DE-Pro MALDI-TOF mass spectrometer (Applied Biosystems, CA, USA). Samples were prepared as previously reported [19] using ferulic acid (FA) matrix dissolved in 20% ACN/0.1% v/v TFA/water at a concentration of 10 mg/mL with 100 mM serine as an additive. The FA/serine combination was shown to be the most efficient matrix for analysis of crude ponerine ant venoms *via* MALDI-TOF MS [19]. Spell 0.5 μL of each sample was deposited on the MALDI target plate followed by 0.5 μL of the FA matrix. Each mass spectrum was externally calibrated using a mixture of peptides of known molecular mass in the same *m/z* range (Peptide Calibration Mix 4, LaserBio Labs, Sophia-Antipolis, France). Lastly, 0.5 μL of the calibration mixture was co-crystallized with 0.5 μL of the matrix and placed adjacent to each sample and analyzed separately. All calibration spectra were acquired in automated mode to maximize mass accuracy and reproducibility. All spectra were acquired in reflector mode and sample spectra were calibrated automatically using the sequence module of the Voyager® Control Software (Applied Biosystems, CA, USA). Five spectra of 50 laser shots per spectrum were accumulated for each sample based on defined acceptance parameters and adequate signal intensity in the 500–10,000 *m/z* range. Mass spectra were collected in positive ion mode with 20 kV acceleration. Signals below 500 *m/z* were not recorded as they were comprised of mostly matrix-related ion clusters.

2.4. Mass spectra analysis

All mass spectra were processed with Data Explorer® 4.11 software (Applied Biosystems, CA, USA) and subjected to baseline correction with a correlation factor of 0.7 and Gaussian smoothing to reduce noise with a 5-point filter width. Supplementary masses resulting from sodium (+22 Da) and potassium (+38 Da) adducts were manually removed from all mass lists. Masses matching within ±1.0 Da in neighboring HPLC fractions were considered to be identical peptides from incomplete separation. Two-dimensional scatter plots, also known as "2D venom landscapes" [20], were constructed using SigmaPlot 12.0 software (Systat, CA, USA). All peptide masses detected in each HPLC fraction were plotted as a function of their *m/z* values (*y*-axis) and their HPLC retention time (*x*-axis), the latter being a reflection of their hydrophobicity.

The number of residues per peptide was estimated using the theoretical average amino acid molecular weight (111.1254 Da) determined using the statistical occurrence of amino acids in proteins, calculated with the formula $C_{4.9384}H_{7.7583}N_{1.3577}S_{0.0417}$.

2.5. Disulfide bond reduction and alkylation

The presence of disulfide-linked peptides in ant venoms was determined *via* chemical reduction of crude venoms and subsequent analysis of HPLC fractions. Disulfide reduction was achieved by mixing 5 μL of crude venom or HPLC fraction with 10 μL of 100 mM ammonium bicarbonate buffer (pH 8) containing 6 M guanidine and 10 mM dithiothreitol (DTT) for 30 min at 56 °C. Prior to MS analysis, reduced venoms or

fractions were desalted using ZipTip® C18 pipette tips (Millipore, Billerica, MA, USA). As chemical reduction results in a mass increase of 2 Da for each disulfide bond, the examination of mass shifts in the mass spectra of native and reduced samples permitted the number of disulfide bonds in the corresponding peptides to be determined. The disulfide-linked peptides were purified and further analyzed after reduction/alkylation to confirm their disulfide-bond content: following reduction with DTT, the peptides were alkylated by incubation in 50 mM iodoacetic acid (IAA) for 15 min at room temperature in the dark.

2.6. Chemistry-based sequencing

Purified peptides were subjected to Edman degradation on an gas-phase sequencer model ABI 492 (Applied Biosystems, CA, USA). The phenylthiohydantoin (PTH) amino acid derivatives generated at each sequence cycle were identified and quantified on-line with an Applied Biosystems Model 140C HPLC system using the Applied Biosystems Model 610 A data analysis system for protein sequencing. The PTH-amino acid standard kit was used and reconstituted according to the manufacturer's instructions. The procedures and reagents were used as recommended by the manufacturer.

2.7. De novo MS-based peptide sequencing

After reduction and alkylation, an aliquot (1/3) of each of the six purified peptides (*i.e.* PONTX-Ae1b; Ae1c; Ae1d; Ae1e; Ae1f and Ae1g) was subjected to *de novo* sequencing using an AB Sciex 5600 TripleTOF 5600 System coupled to a Shimadzu 30 series HPLC system (ABSciex, Concord ON, Canada). LC separation was achieved using a C_{18} column (2.1 × 100 mm, 1.8 μm, 300 Å; Agilent, Santa Clara CA, USA) with a fast gradient of 2–50% solvent B (90% ACN/0.1% formic acid) using a flow rate of 0.15 ml·min^{-1} over 4 min. One full scan cycle of the mass range (300–1800 *m/z*) followed by multiple tandem mass cycles (MS/MS) (80–1400 *m/z*) was applied using a rolling collision energy relative to the *m/z* and charge state of the precursor ion up to a maximum of 80 eV. The full-scan MS had a duration of 14 min with a cycle time of 1.15 s (total of 729 cycles). The maximum number of candidate ions monitored per cycle was 20 and the ion tolerance was 0.1 Da. External calibration was applied before acquisition. All data processing was conducted using Analyst 1.6 software and individual ion spectra were manually interpreted.

2.8. Chemical synthesis

Protected Fmoc-amino acid derivatives were purchased from Novabiochem or Auspep (Melbourne VIC, Australia). The following side chain protected amino acids were used: Cys(Trt), His(Trt), Hyp(tBu), Tyr(tBu), Lys(Boc), Trp(Boc), Arg(Pbf), Asn(Trt), Asp(OtBu), Glu(OtBu), Gln(Trt), Ser(tBu), Thr(tBu), Tyr(tBu). All other Fmoc amino acids were unprotected. Dimethylformamide (DMF), dichloromethane (DCM), diisopropylethylamine (DIEA), and (TFA) were supplied by Auspep as peptide-synthesis grade. 2-(1H-benzotriazol-1-yl)-1,1,3,3-tetramethyluronium hexafluorophosphate (HBTU), triisopropylsilane (TIPS), HPLC-grade acetonitrile, aceticanhydride and methanol were supplied by Sigma Aldrich (St Louis, Missouri, USA). Ethanedithiol (EDT) was supplied by Merck (St Louis, Missouri, USA).

C-terminal amide and C-terminal carboxyl versions of the ant venom peptide Ae1a were synthesized on a Symphony automated peptide synthesizer (Protein Technology, Tucson AZ, USA) using Rink amide resin (0.1 mmol) and Fmoc-Cys-Wang resin (SV = 0.5 mmol/g), respectively. Peptides were assembled using HBTU/DIEA *in situ* activation protocols [21] to couple the Fmoc-protected amino acid to the resin (5 equiv. excess; coupling time 5 min). Fmoc deprotection was performed with 30% piperidine/DMF for 1 min followed by a 2-min repeat. Washes were performed 10 times after each coupling as well as after each deprotection step. After chain assembly and final Fmoc deprotection, the peptide resins were washed with methanol and dichloromethane and dried in a stream of nitrogen. Cleavage of the peptide resin was performed at room temperature in TFA/H_2O/TIPS/EDT (87.5/5/5/2.5) for 3 h. Cold diethyl ether (30 ml) was then added to the cleavage mixture and the peptide precipitated. The precipitate was collected by centrifugation and subsequently washed with further cold diethyl ether to remove scavengers. The final product was dissolved in 50% aqueous ACN/0.1% TFA and lyophilized to yield a solid white product. The crude, reduced peptide was analyzed using RP-HPLC to determine purity, and the correct molecular weight was confirmed using electrospray ionization (ESI) MS.

Purified, reduced amidated and carboxyl forms of Ae1a (1 mg/ml) were oxidized by stirring at room temperature in 10% dimethyl sulfoxide (DMSO)/0.1 M NH_4HCO_3 pH 8.0, for 16 h. The solutions were subsequently diluted to a DMSO concentration < 5% prior to RP-HPLC purification. A single main oxidized product was purified to >95% purity and lyophilized.

Analytical HPLC runs were performed using a Shimadzu HPLC system LC10A (Shimadzu, Kyoto, Japan) with dual wavelength detection at 214 nm and 254 nm. A reversed-phase C_{18} column (Zorbax 300-SB C_{18}; 4.6 × 50 mm, Agilent) was used with a flow rate of 2 ml·min^{-1}. Gradient elution was performed with the following buffer systems: A, 0.05% TFA in water and B, 0.043% TFA in 90% ACN in water, from 0% to 80% B in 20 min. The crude peptides and oxidized peptides were purified by semi-preparative HPLC on a Shimadzu HPLC system LC8A using a 25 cm × 10 mm reversed-phase C_{18} column (Grace, Columbia MD, USA) running at a flow rate of 5 ml·min^{-1} with a 1%/min gradient of 5–50% B. The purity of the final product was evaluated by analytical HPLC (Zorbax 300SB C18, 4.6 × 100 mm, Agilent) using a flow rate of 1 ml·min^{-1} and a 1.67%/min gradient of 5–45% B. The purity of all synthetic peptides was >95%.

Peptide concentrations used during *in vitro* screening were calculated based on peak size detected at 214 nm relative to that of a peptide standard of known concentration established *via* amino acid analysis. Molecular extinction coefficients were calculated for the standard and the peptide of interest by applying increments established by Buck et al. [22].

ESI mass spectra were collected in-line during analytical HPLC runs on an Applied Biosystems API-150 spectrometer operating in positive ion mode with an OR of 20, Rng of 220 and a Turbo spray of 350°. Masses between 300 and 2200 amu were detected (step 0.2 amu, dwell 0.3 ms).

2.9. Peptide structure determination

Two-dimensional homonuclear NMR spectroscopy was used to determine the structure of Ae1a. Lyophilized Ae1a was resuspended at a final concentration of 2 mM in 300 μL of 20 mM sodium phosphate, pH 6 containing 5% D_2O. An additional sample was prepared by lyophilizing the above sample and resuspending it in 100% D_2O. Spectra were acquired at 25 °C on a Bruker AVANCE 600 MHz spectrometer equipped with a cryoprobe (Bruker, Billerica MA, USA). Resonance assignments were obtained using a combination of 2D ^{1}H-^{15}NHSQC, ^{1}H-^{13}CHSQC (in 100% D_2O) and TOCSY spectra. Interproton distance restraints were obtained from a 2D NOESY spectrum acquired with a mixing time of 300 ms. Spectra were processed using Topspin (Version 3.2, Bruker) and analyzed using CcpNmr Analysis 2.4.1 [23]. Chemical shift assignments have been deposited in BioMagResBank (accession number 25971). Dihedral-angle restraints were derived from TALOS+ chemical shift analysis [24] and the restraint range was set to twice the estimated standard deviation. The NOESY spectrum was manually peak picked, then the torsion angle dynamics package CYANA 3 [25] was used to automatically assign the peak list, extract distance restraints, and calculate an ensemble of structures. During the process of automatic NOESY spectrum assignment, CYANA assigned 95.8% of all NOESY cross-peaks. The final structure was calculated using a total of 190 interproton distance restraints, 6 disulfide-bond distance restraints,

and 27 dihedral-angle restraints; 200 structures were calculated and the top 20 were selected on the basis of final CYANA penalty function values and stereochemical quality as judged by MolProbity [26]. Atomic coordinates for the final ensemble of 20 structures are available from the Protein Data Bank (PDB ID 2NBC).

2.10. Insecticidal bioassay

Synthetic Ae1a was dissolved in insect saline [27] and injected into the ventro-lateral thoracic region of sheep blowflies (*Lucilia cuprina*, mass 28.5–30.7 mg), using a 1.0 mL disposable syringe (B-D Ultra Fine, Terumo Medical Corporation, Tokyo, Japan) and a fixed 29 gauge needle fitted to an Arnold manual micro-applicator (Burkard Manufacturing Co-Ltd., Uxbridge, UK). A maximum volume of 2 μL was injected per fly. Thereafter, the flies were individually housed in 2-ml tubes and paralytic activity was determined after 1 h and 24 h. A total of three tests was carried out and, for each test, seven doses of Ae1a ($n = 10$ flies per dose) and the appropriate control (insect saline; $n = 20$ flies each) were used. PD_{50} values were calculated as described previously [28,29].

2.11. Ion channel assays

The effect of Ae1a on a range of voltage- and ligand-gated ion channels was determined by measuring Ca^{2+} responses using a fluorescent imaging plate reader ($FLIPR^{TETRA}$) and cells loaded with Calcium 4 dye (Molecular Devices, Sunnyvale CA, USA). The SH-SY5Y neuroblastoma cell line was used as previously described for assaying the voltage-gated ion channels Ca_V1, Ca_V2, Na_V1 and the ligand-gated α7 nicotinic acetylcholine receptor (nAChR) [30,31]. SH-SY5Y cells were plated at 40,000 cells per well on a 384-well flat clear bottom black plate (Corning, NY, USA) and cultured at 37 °C in a humidified 5% CO_2 incubator for 48 h before assay. The medium was removed and the cells loaded with 20 μL per well of Calcium 4 dye reconstituted in an assay buffer containing (in mM) 140 NaCl, 11.5 glucose, 5.9 KCl, 1.4 $MgCl_2$, 1.2 NaH_2PO_4, 5 $NaHCO_3$, 1.8 $CaCl_2$ and 10 HEPES pH 7.4. Cells were then incubated for 30 min at 37 °C in a humidified 5% CO_2 incubator. For the Ca_V1 assay, 1 μM ω-conotoxin CVID (a Ca_V2 blocker) was added to the dye; for the Ca_V2 assay, 10 μM nifedipine (a Ca_V1 blocker) was added to the dye; and for the α7 nAChR assay, 10 μM PNU-120,596 (an α7 agonist) was added to the dye.

Ca^{2+} fluorescence responses were recorded using excitation and emission wavelengths of 470–495 nm and 515–575 nm, respectively. Responses were recorded for 10 s to set the baseline, 600 s after the addition of either *A. emarginatus* crude venom (10, 1 and 0.1 μg/well) or various concentrations of Ae1a, and for a further 300 s after the addition of various activators (90 mM KCL for the Ca_V1 and Ca_V2 assays, 30 μM choline for the α7 nAChR assay, or 30 μM veratridine for the Na_V1 assay). Maximum fluorescent responses were corrected against baseline and used to plot the intracellular calcium influx. Curve fitting (non-linear regression with log[inhibitor] *versus* normalized response and variable Hill slope) was performed using GraphPad Prism Version 6 (GraphPad Software, San Diego CA, USA).

3. Results

3.1. 2D landscape of A. emarginatus venom

A previous investigation of *Anochetus* spp. crude venoms revealed the presence of numerous peptides cross-linked by one or two disulfide bonds [12]. Our analysis of *A. emarginatus* venom using RP-HPLC coupled to off-line MALDI-TOF MS further highlighted the unusual nature of the venom peptidome compared to previously described ant toxins [14]. First, our LC-MS analysis revealed only 35 masses in the venom (Table 1); second, the peptides were relatively small (1460–2100 Da, which corresponds to peptides containing 13–19 residues) (Fig. 1) and relatively hydrophilic, eluting between 10% and 25% ACN (retention time 15–30 min, Fig. 2A); third, after chemical reduction of each HPLC fraction, a mass shift of +4 Da occurred for almost all of the masses detected, indicating that *A. emarginatus* venom is composed almost entirely of peptides with two disulfide bonds. In contrast, we detected only one linear peptide (*m/z* 1623.58) in *A. emarginatus* venom.

Table 1
Mass fingerprint of *Anochetus emarginatus* venom. Masses in bold indicate the seven poneritoxins that were purified and sequenced in this study. The shaded mass indicates a linear peptide; all other peptides are crosslinked by two disulfide bonds.

Fraction	RT (min)	*m/z* [M+H$^+$]
*F*1	15.3	**1790.64**
*F*2	16.2	**1689.58**
*F*3	16.7	1745.85
*F*4	17.2	1727.80
*F*4	17.2	1850.90
*F*5	18.0	**1733.64**
*F*6	19.2	**1916.96**
*F*7	20.0	1770.80
*F*7	20.0	1926.90
*F*8	20.8	1975.12
*F*9	21.3	1689.80
*F*9	21.3	1828.90
*F*10	21.6	1901.05
*F*11	22.1	1713.80
*F*11	22.1	**1852.79**
*F*11	22.1	2027.08
*F*11	22.1	2099.16
*F*12	22.7	1716.89
*F*12	22.7	1623.58
*F*12	22.7	**1866.81**
*F*12	22.7	2081.11
*F*12	22.7	2057.92
*F*13	24.1	1609.90
*F*13	24.1	1711.04
*F*13	24.1	1850.15
*F*13	24.1	1853.24
*F*13	24.1	2009.26
*F*13	24.1	2027.33
*F*13	24.1	1926.10
*F*14	25.1	2094.15
*F*15	25.9	1462.89
*F*15	25.9	2075.18
*F*16	27.0	1909.07
*F*17	28.0	**1975.74**
*F*18	29.4	1959.01

3.2. Poneritoxin sequences

All ants (>13,000 extant species) are grouped into a single family and consequently we propose to slightly modify the standard nomenclature proposed for naming venom peptides from spiders [32], centipedes [5], and sea anemones [33] and to use the 16 extant subfamilies to classify ant venom peptides. Thus, we use the term "poneritoxin" (abbreviated PONTX) to denote venom peptides from *Anochetus* and other species in the ant subfamily Ponerinae [15]. We purified the seven most abundant disulfide-linked poneritoxins (*i.e.*, PONTX-Ae1a; Ae1b; Ae1c; Ae1d; Ae1e; Ae1f; Ae1g) using a combination of C_{18} and C_4 RP-HPLC. These poneritoxins are the first venom peptides to be isolated from *Anochetus* venom.

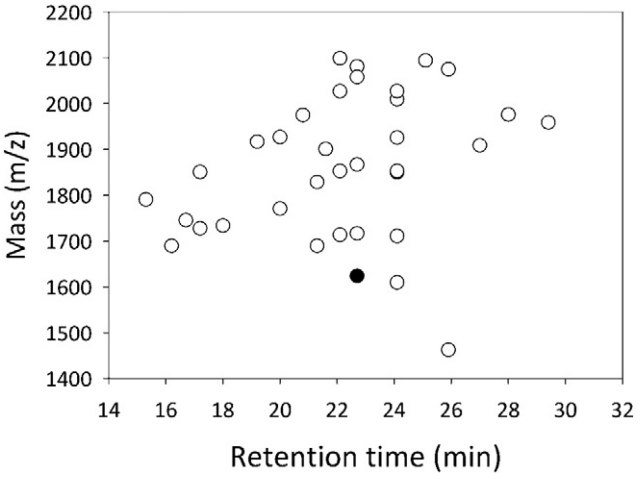

Fig. 1. Venom peptidome of *Anochetus emarginatus*. 2D landscape representation of the venom profile of *A. emarginatus*. Peptide masses from LC-MS analysis are shown on the ordinate axis, while RP-HPLC retention time (a measure of peptide hydrophobicity) is shown on the abscissa. The venom is dominated by peptides with two disulfide bonds (white circles). The black circle indicates the only peptide that was found to lack disulfide bonds.

N-terminal sequencing of Ae1a using Edman degradation yielded the 16-residue sequence WCASGCRKKRHGGCSC, with a calculated mass of 1732.73 Da. Thus, the measured *m/z* value of 1733.64 $[M + H]^+$ for the native peptide is consistent with C-terminal amidation, for which the predicted mass would be 1732.72 Da (Fig. 2). The six remaining purified peptides were subjected to *de novo* MS-based sequencing using a high-resolution AB Sciex Triple TOF 5600 mass spectrometer. Each peptide was individually selected for MS/MS analysis and fragmented by collision-induced dissociation. Sufficient fragmentation and good sequence coverage were obtained for each of the peptides and allowed almost complete sequence characterization. Full sequences were finalized by combining the MS and MS/MS data within information from Edman degradation. Similar to Ae1a, the other six poneritoxins are also C-terminally amidated and are slightly larger than Ae1a, comprising either 18 residues (PONTX-Ae1b, PONTX-Ae1c, PONTX-Ae1d, PONTX-Ae1e and PONTX-Ae1g) or 19 residues (PONTX-Ae1f). They show 40–90% sequence identity with Ae1a. Ae1a, PONTX-Ae1b, PONTX-Ae1c and PONTX-Ae1d are 61–94% identical and are very basic (predicted pI of 9–9.3). PONTX-Ae1g and PONTX-Ae1e are more dissimilar (41–50% identity with Ae1a) and less basic (predicted pI of 8.5–8.6). PONTX-Ae1f is the most hydrophobic of the seven peptides and the least basic (pI ~ 7.5).

An alignment of the sequences of the seven peptides (Table 2) reveals several strictly conserved features, including the four cysteine residues, a glycine immediately preceding the second cysteine, and a doublet of glycine residues preceding the third cysteine residue. The glycine content is unusually high in these peptides, ranging from 16.7% in PONTX-Ae1c and PONTX-Ae1d to 33.3% in Ae1e. These peptides are clearly paralogs, and therefore should be classified in the same isotoxin group, but they have no sequence similarities to any previously described venom peptides. The unique amino acid sequence and cysteine framework of the poneritoxins indicate that they might have a unique 3D fold, and hence we decided to pursue structural characterization of Ae1a.

3.3. Synthesis and NMR structure of PONTX-Ae1a

Synthetic Ae1a was produced by solid-phase peptide synthesis. Oxidation of the synthetic linear peptide resulted in one major peak that coeluted with the native peptide on RP-HPLC, consistent with formation of the correct disulfide-bind isomer. The three-dimensional structure of synthetic Ae1a was elucidated using homonuclear NMR methods.

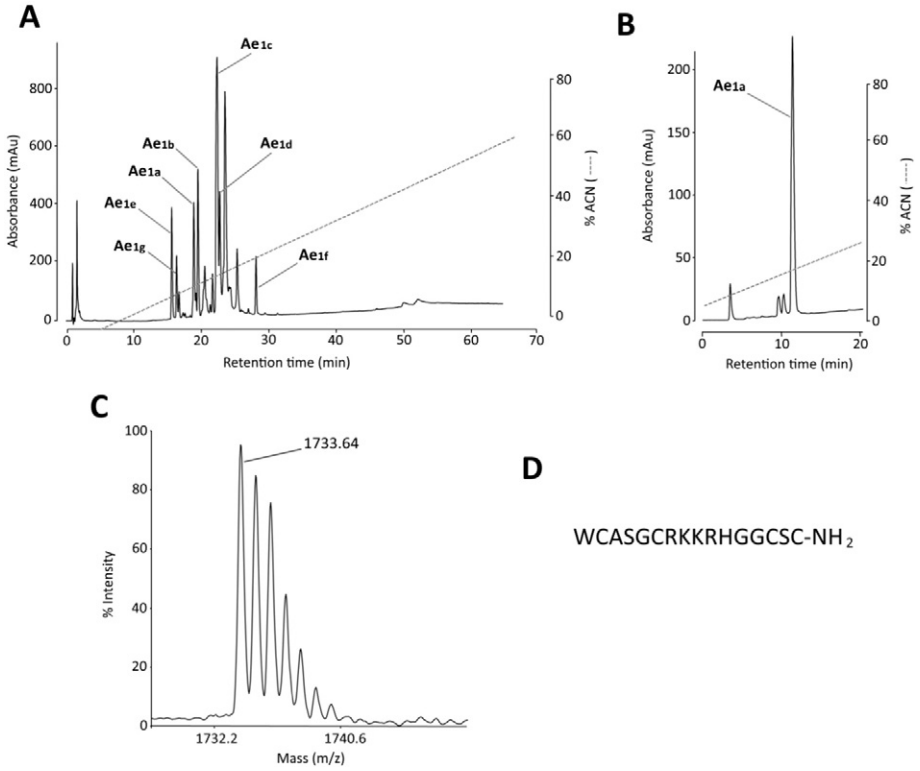

Fig. 2. Isolation of Ae1a. (A) RP-HPLC chromatogram resulting from fractionation of crude venom from *Anochetus emarginatus* on a C_{18} column. Peaks containing the seven peptides that were selected for purification are labeled. (B) Chromatogram showing purification of peptide Ae1a using C_4 RP-HPLC. (C) MALDI-TOF MS spectrum of purified native Ae1a. (D) Amino acid sequence of PONTX-Ae1a determined using Edman degradation and mass spectrometry.

Table 2
Sequence alignment of poneritoxins. Alignment of the seven poneritoxins sequenced in this study. Gaps were introduced to optimize the alignment. Asterisks denote an amidated C-terminus. Percentage identity (% ID) is relative to U_1-PONTX-Ae1a. Theoretical monoisotopic masses were calculated using GPMAW 10.0 software.

Peptide[a]	Sequence	% ID	Mass [M]
U_1-PONTX-Ae1a	---WCASGCRKKRHGG-CSC*	–	1732.73 Da
U_1-PONTX-Ae1b	--RYCPSGCRKKPYGGGCSC*	70.6	1915.80 Da
U_1-PONTX-Ae1c	-RSVCSNGCRPKPFGG-CSC*	62.5	1851.77 Da
U_1-PONTX-Ae1d	-RSLCSNGCRPKPFGG-CSC*	62.5	1865.79 Da
U_1-PONTX-Ae1e	-GVGCSSGCHK--VGGQCRCG*	52.9	1688.68 Da
U_1-PONTX-Ae1f	SFYACTNGCWVKPGGG-CQC*	50.0	1974.76 Da
U_1-PONTX-Ae1g	-GTGCSSGCHR--VGQQCRCG*	41.2	1789.70 Da

[a] Standard nomenclature system for naming ant-venom peptides [15].

Fig. 3B shows a stereoview of the ensemble of 20 conformers representing the solution structure of PONTX-Ae1a. The disulfide connectivity for PONTX-Ae1a was determined by performing three separate structure calculations with the three possible disulfide isomers (*i.e.*, Cys^2–Cys^{14}/Cys^6–Cys^{16}; Cys^2–Cys^6/Cys^{14}–Cys^{16}; and Cys^2–Cys^{16}/Cys^6–Cys^{14}). Only the Cys^2–Cys^{14}/Cys^6–Cys^{16} connectivity was consistent with the pattern of NOEs seen in the NOESY spectrum and this connectivity was the only one to yield no restraint violations in the structure calculations. We therefore infer this to be the native disulfide connectivity for Ae1a.

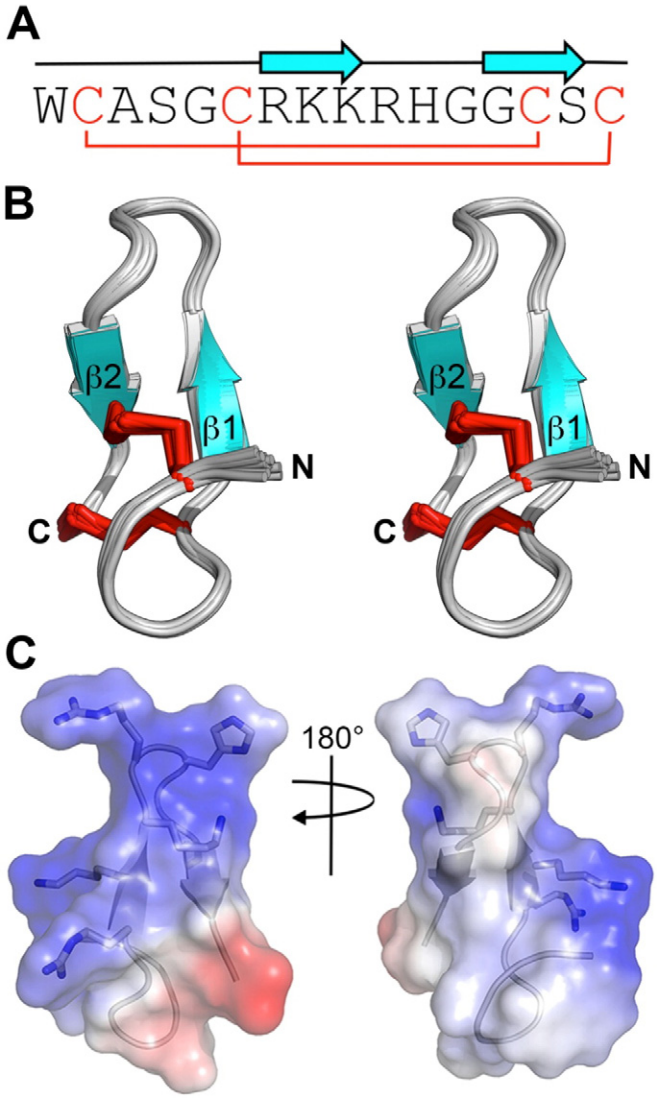

Fig. 3. Solution structure of Ae1a (PDB: 2NBC). (A) Primary structure of Ae1a. The secondary structure of Ae1a determined from the NMR-derived solution structure is shown above the sequence, with β-strands denoted by cyan arrows. Disulfide bonds are highlighted in red. (B) Stereoview of the ensemble of 20 structures of Ae1a overlaid for best fit over the backbone atoms of residues 2–16. β-Strands are colored cyan and the two disulfide bonds are shown as red tubes. (C) Electrostatic surface of Ae1a. Positively- and negatively-charged regions are shown in blue and red, respectively. The side chains are displayed for residues that contribute to the positively-charged surface.

The structural statistics for the ensemble of PONTX-Ae1a structures are summarized in Table 3. The structure is highly precise, with a backbone rmsd of 0.17 ± 0.04 Å over residues 2–16. The stereochemical quality of the structure is also very high, with MobProbity analysis revealing a complete absence of steric clashes and 93.6% of residues in the most favored region of the Ramachandran plot. The structure ranks as high-resolution based on these measures of precision and stereochemical quality [34].

Ae1a forms a compact structure in which a C-terminal β-hairpin is connected to the N-terminal region *via* the two disulfide bonds. This two-disulfide structure appears to be a novel fold that has not been previously reported for any other toxin. A DALI comparison with the PDB was not possible because of the small size of the toxin (the cut-off size for DALI analysis is 20 residues). Mapping the electrostatic potential onto the surface of Ae1a (Fig. 3C) revealed that the C-terminal β-hairpin is highly cationic, with two positively charged residues emanating from β-strand 1 (Arg^7/Lys^8) and three from the β-hairpin loop (Lys^9/Arg^{10}/His^{11}). It remains to be determined whether this is linked to the inherent biological activity of the toxin.

3.4. Insecticidal activity

Injection of synthetic Ae1a into sheep blowflies (*Lucilia cuprina*) resulted in paralysis; the PD_{50} measured 1 h after injection was 8.9 ± 3.1 nmol/g (Fig. 4). The activity of the toxin was completely reversible and all of the flies recovered within 24 h following injection. No lethal effects of Ae1a were observed within the dose range tested.

3.5. Effects on human ion channels

Crude venom from *A. emarginatus* was screened in a FLIPR-based assay to examine potential activity against human voltage-gated calcium (Ca_V) and sodium (Na_V) channels as well the ligand-gated α7 nAChR endogenously expressed in SH-SY5Y cells. These pharmacological targets are of particular interest for the development of therapeutic agents and are currently part of intense screening programs to find

Table 3
Statistics for the ensemble of U_1-PONTX-Ae1a structures[a].

Experimental restraints[b]	
Interproton distance restraints-Total	190
Intraresidue ($\|i–j\| < 0$)	50
Sequential ($\|i–j\| \leq 1$)	64
Medium range ($1 < \|i–j\| < 5$)	35
Long range ($\|i–j\| >= 5$)	41
Disulfide-bond restraints	6
Dihedral-angle restraints (φ, ψ)	27
Total number of restraints per residue	11.9
R.m.s. deviation from mean coordinate structure (Å)	
Backbone atoms (residues 2–16)	0.17 ± 0.04
All heavy atoms (residues 2–16)	0.93 ± 0.14
Stereochemical quality[c]	
Residues in most favored Ramachandran region (%)	93.6 ± 2.2
Ramachandran outliers (%)	0 ± 0
Unfavorable side chain rotamers (%)	4.2 ± 4.3
Clashscore, all atoms[d]	0 ± 0
Overall MolProbity score	1.3 ± 0.4

[a] All statistics are given as mean ± S.D.
[b] Only structurally relevant restraints, as defined by CYANA, are included.
[c] According to MolProbity (http://molprobity.biochem.duke.edu).
[d] Defined as the number of steric overlaps >0.4 Å per thousand atoms.

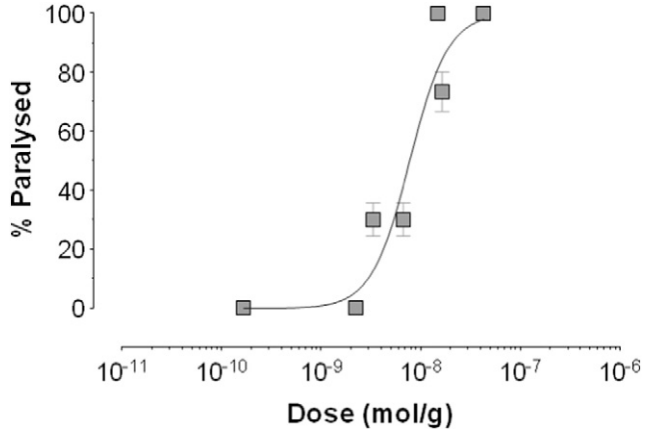

Fig. 4. Insecticidal potency of Ae1a. Dose-response curve resulting from injection of Ae1a into sheep blowflies (*Lucilia cuprina*). Data points are mean ± SEM. The percentage of paralyzed blowflies was determined after 1 h, and the median paralytic dose (PD_{50}) was determined from the average ± SEM of three independent experiments.

selective agonists and antagonists. No activity was observed against Na_V1, Ca_V2 channels, or the α7 nAChR (data not shown) but the crude venom inhibited calcium entry *via* Ca_V1 channels (Fig. 5A). Moreover, synthetic Ae1a completely abolished the Ca_V1 response in SH-SY5Y cells with an IC_{50} of 4.6 μM (Fig. 5B). Interestingly, the activity of Ae1a against Ca_V1 channels was completely dependent on C-terminal amidation (Fig. 5C), indicating that the C-terminus of Ae1a plays a crucial role in its interaction with this ion channel.

4. Discussion

Ant venom represents an untapped resource for the discovery of peptides with novel pharmacology and structure. 3D structures have been reported for only two ant-venom peptides, namely the heterodimeric, three-disulfide ectatomin from *Ectatomma tuberculatum* [46] and poneratoxin, a 25-residue linear peptide from *Paraponera clavata* [47]. A previous study highlighted that several ant venoms from the genus *Anochetus* were almost entirely composed of small peptides with one or two disulfide bonds [12]. Since two-disulfide peptides have been seldom described, we deemed the potential for discovery of a novel toxin scaffold from the venom of *Anochetus emarginatus* to be very high.

Determination of the structure of one of the poneritoxins from *A. emarginatus*, Ae1a, revealed a unique β-hairpin fold stabilized by two disulfide bonds. Animal venom peptides are often structured by multiple disulfide bonds and therefore exhibit a wide variety of folds. Except for cone snail venoms (*e.g.*, α-conotoxins; [35]), small venom peptides (<30 aa) structured by two disulfide bonds are rare in other venomous animals, although they have been occasionally noted in venoms from hymenopterans (*e.g.*, apamin, tertiapin, MCDP [36–38]), and snakes (*e.g.*, sarafotoxins [39]). There is no significant sequence or structural homology between these toxins and the poneritoxins described in the current study (Table 4). Fig. 6 shows that, in striking contrast with Ae1a, the secondary structures of most small two disulfide-bonded peptides are dominated by α-helices (*e.g.*, tertiapin, sarafotoxin, and α- and ρ-conotoxins) [40–43]. However, despite very distinctive amino acid sequences, the secondary and tertiary structures of Ae1a and χ-conotoxin MrIA are quite similar (compare Fig. 6A and B). χ-Conotoxin MrIA is a 13-residue peptide isolated from the venom of *Conus marmoreus* that inhibits the norepinephrine transporter [41]. Both toxins have a β-hairpin motif with two antiparallel strands connected by a turn. Nevertheless, the cysteine frameworks of Ae1a and χ-conotoxin MrIA (C-C-C-C and CC-C-C, respectively) and their disulfide connectivities (C_1-C_3, C_2-C_4 and C_1-C_4, C_2-C_3, respectively) are quite different. Thus, we conclude that 3D structure of Ae1a is distinctly different

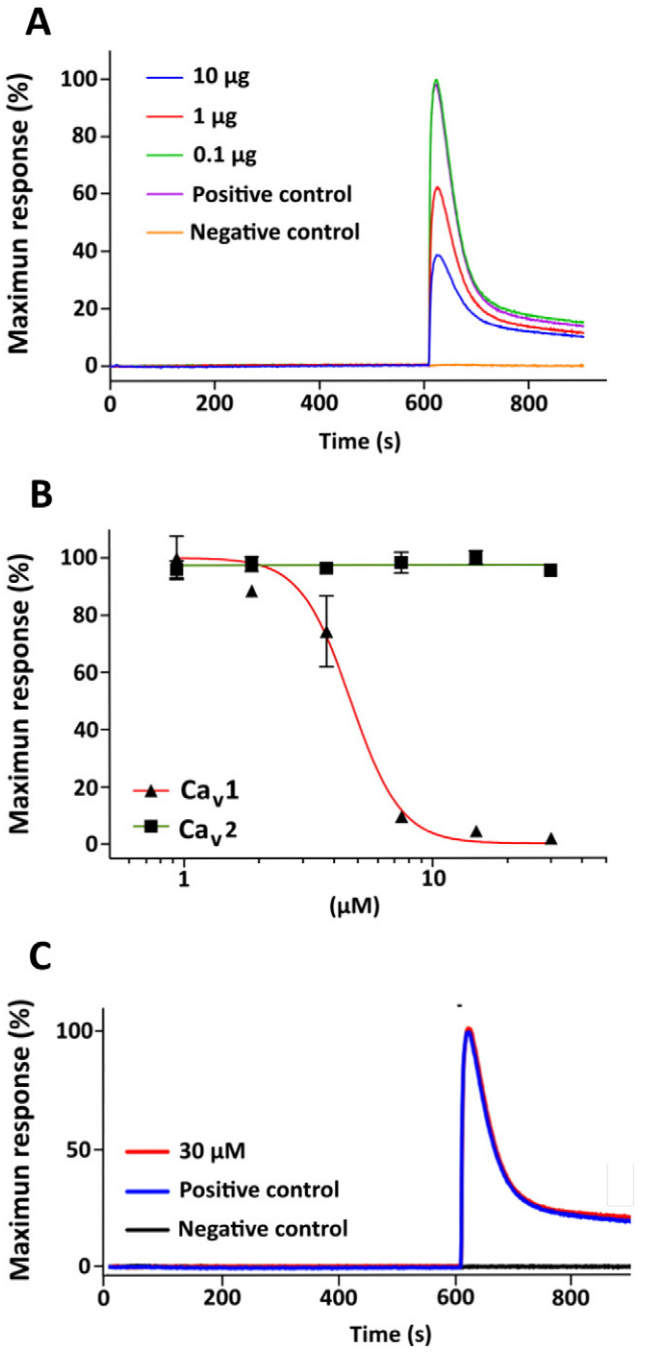

Fig. 5. Activity of *Anochetus emarginatus* venom and Ae1a peptide against channels endogenously expressed in SH-SY5Y cells. (A) Crude venom was reconstituted in assay buffer and applied at 10, 1 and 0.1 μg/well to SH-SY5Y cells loaded with Calcium 4 dye in the presence of 1 μM ω-conotoxin CVID (Ca_V2 blocker). After 10 min incubation with the venom, cells were activated with 90 mM KCl and the intracellular calcium responses recorded. *A. emarginatus* venom reduced the Ca_V1 response to 60% and 40% at concentrations of 10 and 1 μg/well, respectively, but was inactive at a dose of 0.1 μg/well. (B) Dose-response curves for the modulation of Ca_V1 and Ca_V2 responses in SH-SY5Y cells by Ae1a. Synthetic Ae1a inhibited the Ca_V1 response with an IC_{50} of 4.6 μM, but had no effect on Ca_V2. (C) At a concentration of 30 μM the non-amidated form of Ae1a caused no inhibition of Ca_V1 responses in SH-SY5Y cells.

from other venom peptides, including all known Ca_V channel toxins, thus providing a new scaffold for drug design and protein engineering applications.

Ae1a is a moderately potent insecticidal peptide toxin, having a PD_{50} that is about 40-fold higher than the LD_{50} reported for the most potent insecticidal spider venom peptides that we have tested using the same

Table 4
Sequences of small venom peptides reticulated by two disulfide bonds. Percentage identity (% ID) is relative to the first peptide (U_1-PONTX-Ae1a). Asterisk denotes C-terminal amidation.

Peptide	Specie	Sequence	% ID	Target
U_1-PONTX-Ae1a	*Anochetus emarginatus*	WCASGCRKKRHGGCSC*	–	Ca_v channel
Apamin	*Apis mellifera*	--CNCKAPETAL--CARRCQQH*	15	K_v channel
Tertiapin	*Apis mellifera*	ALCNCNRIIIPHM-CWKKCGKK*	23.8	K_v channel
MCDP	*Apis mellifera*	IKCNCKRHVIKPHICRKICGKN*	22.7	K_v channel
Sarafotoxin 6b	*Atractaspis engaddensis*	CSCKDMTDKECLTFCHQDVIW	15	Endothelin receptor
α-Conotoxin AuIB	*Conus aulicus*	---GCCSYPPCFATNPD-C*	17.6	Nicotinic receptor
α-Conotoxin EI	*Conus ermineus*	-RDOCCYHPTCNMSNPQIC*	17.6	Nicotinic receptor
α-Conotoxin GI	*Conus geographus*	---ECCNPA-CGRHYS--C*	18.8	Nicotinic receptor
α-Conotoxin IMI	*Conus imperialis*	---GCCSDP-CAWR----C*	17.6	Nicotinic receptor
α-Conotoxin MII	*Conus magus*	---GCCSNPVCHLEHSNLC*	17.6	Nicotinic receptor
α-Conotoxin PnIB	*Conus pennaceus*	---GCCSLPPCAANNPDYC*	17.6	Nicotinic receptor
α-Conotoxin PIA	*Conus purpurascens*	-RDPCCSNPVCTVHNPQIC*	17.6	Nicotinic receptor
α-Conotoxin SI	*Conus striatus*	---ICCNPA-CGPKTS--C*	25.1	Nicotinic receptor
ρ-Conotoxin TIA	*Conus tulipa*	FNWRCCLIPACRRNHKKFC*	23.5	Adrenergic receptor
χ-Conotoxin MrIA	*Conus marmoreus*	-NGVCCGYKLCHO-----C	18.2	Noradrenalin receptor

assay [44,45]. Nevertheless, the ability of Ae1a to induce fast and completely reversible paralysis in insects could make it an interesting lead molecule for the development of bioinsecticides that aim to minimize effects on beneficial insect species. While spraying such a reversible bioinsecticide on a broad-acre crop would initially paralyse all targeted insect species, most of them would recover and only pest insects that continued to consume the crop would get entangled in a cycle of paralysis-recovery-consumption-paralysis. This would make these insects easy prey for predatory arthropod species and also inhibit their growth, ultimately leading to death. Reversibly paralytic insecticides would also be ideal for expression in transgenic plants [46], targeting only those pests that continuously consume them.

Ion channels are the most common molecular target of disulfide-rich neurotoxic peptides from arthropod venoms [47,48]. Ca_V channels in particular are targeted by many venom peptides with diverse selectivity for both vertebrate and invertebrates [49–51]. Here, we demonstrated that Ae1a blocks vertebrate L-type Ca_V channels (Ca_V1), albeit with low potency (IC_{50} ~ 4.6 μM). Interestingly, very few venom peptides have been characterized that modulate the activity of vertebrate L-type calcium channels. Calciseptine and calcicludine, isolated from the venoms of the black mamba (*Dendroaspis polylepis*) and green mamba (*D. angusticeps*) respectively, block vertebrate Ca_V1 channels [51,52]. Peptide toxins CSTX-1 and ω-TRTX-Cc1a isolated from venoms of the spiders *Cupiennius salei* and *Pelinobius muticus* respectively, are selective inhibitors of Ca_v1 channels [53,54]. Among ants, the heterodimeric peptide Et-1 from *Ectatomma tuberculatum* venom is capable of inhibiting whole-cell L-type calcium currents in isolated rat ventricular myocytes [17]. These other toxins that modulate that activity of Ca_V1 channels have no significant sequence or structural homology with Ae1a.

In this study, we cannot assume that Ae1a also targets insect Ca_V channels because it has low potency against vertebrate Ca_v1 channels. Considering that the level of identity between insect Ca_V channels and their closest human ortholog is only ~66% [55], this paucity of venom peptides with activity against vertebrate Ca_V channels is perhaps not surprising. Ae1a could possibly have more profound effects on insect Ca_V channels or other types of insect ion channels. More extended pharmacological studies using insect neurons are therefore required to determine the ecologically relevant molecular target of Ae1a in insects. Following the rational nomenclature rules for venom peptides, this

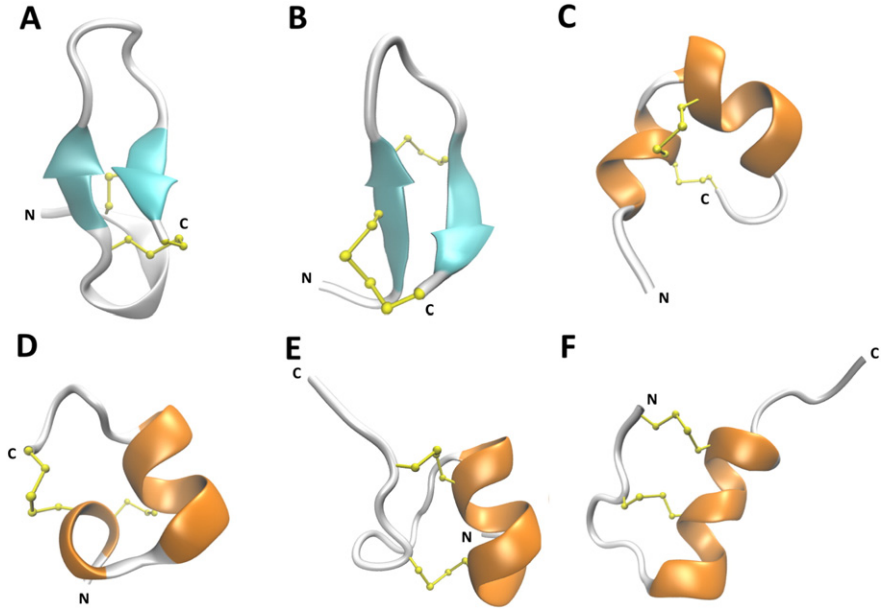

Fig. 6. Comparison of the structure of Ae1a with other small two-disulfide venom peptides. (A-F) Ribbon representations of the 3D structures of (A) Ae1a (PDB 2NBC); (B) χ-Conotoxin MrIA (PDB 2EW4); (C) ρ-Conotoxin TIA (PDB 2LR9); (D) α-Conotoxin MII (PDB 1M2C); (E) Tertiapin (PDB 1TER); (F) Sarafotoxin 6b (PDB 1SRB). Disulfide bonds are indicated by yellow sticks and spheres, while β-strands and α-helices are highlighted by respectively cyan arrows and orange helices.

toxin should be named U_1-PONTX-Ae1a, since the prefix "U" indicates that the pharmacological target is not known [32].

From an evolutionary perspective, the venom peptidome presented in this study is intriguing. Our data reveal that *A. emarginatus* venom, and potentially venom from other *Anochetus* species, have unique features compared to the venom from other stinging ants [14]. First, the venom is unusual for ants in being composed almost entirely of disulfide-linked peptides. Second, *A. emarginatus* venom is simpler than other ant venoms as it contains only 35 peptides, whereas >300 peptides were found in venom from the related ponerine species *Dinoponera quadriceps* [13]. Third, almost all of the poneritoxins found in *A. emarginatus* venom contain two disulfide bonds and are similar in size (13–19 residues), suggestive of divergent evolution from a single ancestral gene.

None of the poneritoxins characterized here have homology to known venom peptides from ants or other venomous animals. The seven poneritoxins are paralogs, containing a conserved disulfide scaffold ($CX_3CX_{6-8}CX_1C$) with either minor differences in their amino acid sequence (*e.g.*, PONTX-Ae1c and PONTX-Ae1d differ by only one residue), or quite divergent primary structures (*e.g.*, PONTX-Ae1f). Presumably, this divergence of sequence suggests a range of potency, selectivity, and/or diverse modes of action among these toxins as is often observed in other arthropod venoms in which subclasses of toxins from a single venom simultaneously target various pharmacological classes of receptors to enhance venom efficacy. As the number of peptides detected in *A. emarginatus* venom is comparatively small, it would nevertheless be expected that structural divergence originating from a very limited set of genes could allow for the diversification of the pharmacological activities and efficacy of the venom.

Based on examination of the 2D venom landscapes of both *Anochetus* and *Odontomachus*, the venom composition and structural diversity appear to be quite dissimilar [56,57]. These closely related ant genera share morphological and behavioral features: they both use their trapjaws to capture prey, followed by a paralyzing sting. However, the poneritoxins described here from *A. emarginatus* diverge significantly from the venom peptides found in six species of the sister genus *Odontomachus* which are dominated by linear peptides with only a minor proportion of toxins containing one disulfide bond [12,19]. This suggests rapid diversification of their venoms since these genera separated ~30 Mya, presumably in response to ecological cues [58]. It will be interesting in future studies to compare the venom peptidome of *A. emarginatus* with that of *Anochetus* and *Odontomachus* species that inhabit vastly different ecological niches, such as ground-dwelling species and species that have very different diets.

5. Conclusions

In summary, our data suggest that *Anochetus* have evolved a novel molecular strategy for the chemical immobilization of prey. The unique β-hairpin fold found in *Anochetus* poneritoxins has presumably contributed to the evolutionary success of this genus, which is abundant and widespread in tropical and subtropical regions of the world. Exploration of the 34 other poneritoxins reported here, as well as novel poneritoxins found in venom from the 114 currently described *Anochetus* species [11], will undoubtedly lead to the discovery of novel ion channel ligands as well as lead molecules for the discovery of novel drugs and bioinsecticides.

Conflict of interest

The authors declare that they have no conflict of interest with the contents of this article.

Author contributions

AT conceived and wrote the manuscript, conducted ant collection, venom gland dissections and most of proteomic experiments. AB and PFA conducted the chemical synthesis. FCC conducted pharmacological experiments. YKYC and GFK conducted and analyzed NMR experiments. VH conducted insecticidal bioassays. AHJ conducted MS/MS experiments. AD, JO and PE conceived the idea for the project. All authors provided comments on the manuscript.

Transparency document

The Transparency document associated with this article can found, in online version.

Acknowledgements

We are grateful to Dr. Jacques Delabie for the identification of ants, to Andrea Yockey-Dejean for proofreading the manuscript, and to Geoff Brown (Department of Agriculture, Fisheries and Forestry, Brisbane) for supplying blowflies. We thank Jean-Pierre Andrieu, from the IBS platform of the Partnership for Structural Biology and the Institut de Biologie Structurale in Grenoble (PSB/IBS), for assistance and access to the Protein Sequencing Facility. Financial support for this study was provided by the *Programme Convergence* 2007-2013, *Région Guyane* from the European community (BI-Appli, 115/SGAR-DE/2011/052274), an *Investissement d'Avenir* grant managed by the *Agence Nationale de la Recherche* (CEBA, ANR-10-LABX-25-01; project AntPep) and Discovery Grant DP130103813 to G.F.K. from the Australian Research Council. G.F.K. and P.F.A. are supported by Principal Research Fellowships from the Australian National Health & Medical Research Council.

References

[1] N.R. Casewell, W. Wüster, F.J. Vonk, R.A. Harrison, B.G. Fry, Complex cocktails: the evolutionary novelty of venoms, Trends Ecol. Evol. 28 (2013) 219–229.
[2] G. Habermehl, Venomous Animals and Their Toxins, Springer Science & Business Media, New York, NY, USA, 2012.
[3] G.F. King, M.C. Hardy, Spider-venom peptides: structure, pharmacology, and potential for control of insect pests, Annu. Rev. Entomol. 58 (2013) 475–496.
[4] R.C. Rodríguez de la Vega, E.F. Schwartz, L.D. Possani, Mining on scorpion venom biodiversity, Toxicon 56 (2010) 1155–1161.
[5] E.A. Undheim, A. Jones, K.R. Clauser, J.W. Holland, S.S. Pineda, G.F. King, B.G. Fry, Clawing through evolution: toxin diversification and convergence in the ancient lineage Chilopoda (centipedes), Mol. Biol. Evol. 31 (2014) 2124–2148.
[6] E.P. Cherniack, Bugs as drugs, part two: worms, leeches, scorpions, snails, ticks, centipedes, and spiders, Altern. Med. Rev. 16 (2011) 50–58.
[7] B.M. von Reumont, L.I. Campbell, S. Richter, L. Hering, D. Sykes, J. Hetmank, R.A. Jenner, C. Bleidorn, A polychaete's powerful punch: venom gland transcriptomics of *Glycera* reveals a complex cocktail of toxin homologs, Genome Biol. Evol. 6 (2014) 2406–2423.
[8] B.M. von Reumont, A. Blanke, S. Richter, F. Alvarez, C. Bleidorn, R.A. Jenner, The first venomous crustacean revealed by transcriptomics and functional morphology: remipede venom glands express a unique toxin cocktail dominated by enzymes and a neurotoxin, Mol. Biol. Evol. 31 (2014) 48–58.
[9] S. Yang, Z. Liu, Y. Xiao, Y. Li, M. Rong, S. Liang, Z. Zhang, H. Yu, G.F. King, R. Lai, Chemical punch packed in venoms makes centipedes excellent predators, Mol. Cell. Proteomics 11 (2012) 640–650.
[10] B. von Reumont, L. Campbell, R. Jenner, Quo Vadis Venomics? A roadmap to neglected venomous invertebrates, Toxins 6 (2014) 3488–3551.
[11] AntCatAvailaible online : http://www.antcat.org (accessed on 05 October 2015).
[12] A. Touchard, J.M.S. Koh, S.R. Aili, A. Dejean, G.M. Nicholson, J. Orivel, P. Escoubas, The complexity and structural diversity of ant venom peptidomes is revealed by mass spectrometry profiling, Rapid Commun. Mass Spectrom. 29 (2015) 385–396.
[13] C.T. Cologna, J.d.S. Cardoso, E. Jourdan, M. Degueldre, G. Upert, N. Gilles, A.P.T. Uetanabaro, E.M. Costa Neto, P. Thonart, E. de Pauw, Peptidomic comparison and characterization of the major components of the venom of the giant ant *Dinoponera quadriceps* collected in four different areas of Brazil, J. Proteome 94 (2013) 413–422.
[14] S.R. Aili, A. Touchard, P. Escoubas, M.P. Padula, J. Orivel, A. Dejean, G.M. Nicholson, Diversity of peptide toxins from stinging ant venoms, Toxicon 92 (2014) 166–178.
[15] A. Touchard, S.R. Aili, E.G.P. Fox, P. Escoubas, J. Orivel, G.M. Nicholson, A. Dejean, The biochemical toxin arsenal from ant venoms, Toxins 8 (2016) 30.
[16] A. Duval, C.O. Malecot, M. Pelhate, T. Piek, Poneratoxin, a new toxin from an ant venom, reveals an interconversion between two gating modes of the Na channels in frog skeletal muscle fibres, Pflugers Arch. 420 (1992) 239–247.

[17] K. Pluzhnikov, E. Nosyreva, L. Shevchenko, Y. Kokoz, D. Schmalz, F. Hucho, E. Grishin, Analysis of ectatomin action on cell membranes, Eur. J. Biochem. 262 (1999) 501–506.
[18] K.A. Pluzhnikov, D.E. Nol'de, S.M. Tertyshnikova, S.V. Sukhanov, A.G. Sobol, M. Torgov, A.K. Filippov, A.S. Arsen'ev, E.V. Grishin, Structure activity study of the basic toxic component of venom from the ant *Ectatomma tuberculatum*, Bioorg. Khim. 20 (1994) 857–871.
[19] A. Touchard, M. Dauvois, M.-J. Arguel, F. Petitclerc, M. Leblanc, A. Dejean, J. Orivel, G.M. Nicholson, P. Escoubas, Elucidation of the unexplored biodiversity of ant venom peptidomes via MALDI–TOF mass spectrometry and its application for chemotaxonomy, J. Proteome 105 (2014) 217–231.
[20] P. Escoubas, B. Sollod, G.F. King, Venom landscapes: mining the complexity of spider venoms via a combined cDNA and mass spectrometric approach, Toxicon 47 (2006) 650–663.
[21] P. Alewood, D. Alewood, L. Miranda, S. Love, W. Meutermans, D. Wilson, Rapid in situ neutralization protocols for Boc and Fmoc solid-phase chemistries, Methods Enzymol. 289 (1997) 14.
[22] M.A. Buck, T.A. Olah, C.J. Weitzmann, B.S. Cooperman, Protein estimation by the product of integrated peak area and flow rate, Anal. Biochem. 182 (1989) 295–299.
[23] W.F. Vranken, W. Boucher, T.J. Stevens, R.H. Fogh, A. Pajon, M. Llinas, E.L. Ulrich, J.L. Markley, J. Ionides, E.D. Laue, The CCPN data model for NMR spectroscopy: development of a software pipeline, Proteins: Struct., Funct., Bioinf. 59 (2005) 687–696.
[24] Y. Shen, F. Delaglio, G. Cornilescu, A. Bax, TALOS+: a hybrid method for predicting protein backbone torsion angles from NMR chemical shifts, J. Biomol. NMR 44 (2009) 213–223.
[25] P. Güntert, Automated NMR structure calculation with CYANA, Protein NMR Techniques, Springer 2004, pp. 353–378.
[26] V.B. Chen, W.B. Arendall III, J.J. Headd, D.A. Keedy, R.M. Immormino, G.J. Kapral, L.W. Murray, J.S. Richardson, D.C. Richardson, MolProbity: all-atom structure validation for macromolecular crystallography, Acta Crystallogr., Sect. D 66 (2010) 12–21.
[27] M. Eitan, E. Fowler, R. Herrmann, A. Duval, M. Pelhate, E. Zlotkin, A scorpion venom neurotoxin paralytic to insects that affects sodium current inactivation: purification, primary structure, and mode of action, Biochemistry 29 (1990) 5941–5947.
[28] V. Herzig, W.C. Hodgson, Neurotoxic and insecticidal properties of venom from the Australian theraphosid spider *Selenotholus foelschei*, Neurotoxicology 29 (2008) 471–475.
[29] N.S. Bende, E. Kang, V. Herzig, F. Bosmans, G.M. Nicholson, M. Mobli, G.F. King, The insecticidal neurotoxin Aps III is an atypical knottin peptide that potently blocks insect voltage-gated sodium channels, Biochem. Pharmacol. 85 (2013) 1542–1554.
[30] I. Vetter, C.A. Mozar, T. Durek, J.S. Wingerd, P.F. Alewood, M.J. Christie, R.J. Lewis, Characterisation of Na_v types endogenously expressed in human SH-SY5Y neuroblastoma cells, Biochem. Pharmacol. 83 (2012) 1562–1571.
[31] S.R. Sousa, I. Vetter, L. Ragnarsson, R.J. Lewis, Expression and pharmacology of endogenous Ca_v channels in SH-SY5Y human neuroblastoma cells, PLoS One 8 (2013), e59293.
[32] G.F. King, M.C. Gentz, P. Escoubas, G.M. Nicholson, A rational nomenclature for naming peptide toxins from spiders and other venomous animals, Toxicon 52 (2008) 264–276.
[33] J.S. Oliveira, D. Fuentes-Silva, G.F. King, Development of a rational nomenclature for naming peptide and protein toxins from sea anemones, Toxicon 60 (2012) 539–550.
[34] A.H. Kwan, M. Mobli, P.R. Gooley, G.F. King, J.P. Mackay, Macromolecular NMR spectroscopy for the non-spectroscopist, FEBS J. 278 (2011) 687–703.
[35] H. Terlau, B.M. Olivera, Conus venoms: a rich source of novel ion channel-targeted peptides, Physiol. Rev. 84 (2004) 41–68.
[36] A. Argiolas, P. Herring, J.J. Pisano, Amino acid sequence of bumblebee MCD peptide: a new mast cell degranulating peptide from the venom of the bumblebee *Megabombus pennsylvanicus*, Peptides 6 (1985) 431–436.
[37] J. Gauldie, J.M. Hanson, F.D. Rumjanek, R.A. Shipolini, C.A. Vernon, The peptide components of bee venom, Eur. J. Biochem. 61 (1976) 369–376.
[38] R. Hider, U. Ragnarsson, A comparative structural study of apamin and related bee venom peptides, Biochim. Biophys. Acta 667 (1981) 197–208.
[39] C. Takasaki, N. Tamiya, A. Bdolah, Z. Wollberg, E. Kochva, Sarafotoxins S6: several isotoxins from *Atractaspis engaddensis* (burrowing asp) venom that affect the heart, Toxicon 26 (1988) 543–548.
[40] G.E. Cartier, D. Yoshikami, W.R. Gray, S. Luo, B.M. Olivera, J.M. McIntosh, A new-conotoxin which targets 32 nicotinic acetylcholine receptors, J. Biol. Chem. 271 (1996) 7522–7528.
[41] I.A. Sharpe, J. Gehrmann, M.L. Loughnan, L. Thomas, D.A. Adams, A. Atkins, E. Palant, D.J. Craik, D.J. Adams, P.F. Alewood, Two new classes of conopeptides inhibit the α1-adrenoceptor and noradrenaline transporter, Nat. Neurosci. 4 (2001) 902–907.
[42] X. Xu, J.W. Nelson, Solution structure of tertiapin determined using nuclear magnetic resonance and distance geometry, Proteins: Struct., Funct., Bioinf. 17 (1993) 124–137.
[43] A.R. Atkins, R.C. Martin, R. Smith, ^{1}H NMR studies of sarafotoxin SRTb, a nonselective endothelin receptor agonist, and IRL 1620, an ETB receptor-specific agonist, Biochemistry 2026-2033 (1995) 34.
[44] E.A. Undheim, L.L. Grimm, C.-F. Low, D. Morgenstern, V. Herzig, P. Zobel-Thropp, S.S. Pineda, R. Habib, S. Dziemborowicz, B.G. Fry, Weaponization of a hormone: convergent recruitment of hyperglycemic hormone into the venom of arthropod predators, Structure 23 (2015) 1283–1292.
[45] N.S. Bende, S. Dziemborowicz, M. Mobli, V. Herzig, J. Gilchrist, J. Wagner, G.M. Nicholson, G.F. King, F. Bosmans, A distinct sodium channel voltage-sensor locus determines insect selectivity of the spider toxin Dc1a, Nat. Commun. 5 (2014) 4350.
[46] V. Herzig, N.S. Bende, M.S. Alam, H.W. Tedford, R.M. Kennedy, G.F. King, Methods for deployment of spider venom peptides as bioinsecticides, in: S.D. Tarlochan, S.G. Sarjeet (Eds.), Advances in Insect Physiology, Vol. 47, Academic Press, London, UK 2014, pp. 389–411.
[47] A. Harvey, A. Anderson, E. Rowan, Toxins affecting ion channels, Natural and Synthetic Neurotoxins, Academic Press, London, New York 1993, pp. 129–185.
[48] S. Mouhat, B. Jouirou, A. Mosbah, M. De Waard, J. Sabatier, Diversity of folds in animal toxins acting on ion channels, Biochem. J. 378 (2004) 717–726.
[49] G.F. King, Modulation of insect Ca_v channels by peptidic spider toxins, Toxicon 49 (2007) 513–530.
[50] B.M. Olivera, L.J. Cruz, V. De Santos, G. LeCheminant, D. Griffin, R. Zeikus, J.M. McIntosh, R. Galyean, J. Varga, Neuronal calcium channel antagonists. Discrimination between calcium channel subtypes using ω-conotoxin from *Conus magus* venom, Biochemistry 26 (1987) 2086–2090.
[51] J.R. de Weille, H. Schweitz, P. Maes, A. Tartar, M. Lazdunski, Calciseptine, a peptide isolated from black mamba venom, is a specific blocker of the L-type calcium channel, Proc. Natl. Acad. Sci. U. S. A. 88 (1991) 2437–2440.
[52] H. Schweitz, C. Heurteaux, P. Bols, D. Moinier, G. Romey, M. Lazdunski, Calcicludine, a venom peptide of the Kunitz-type protease inhibitor family, is a potent blocker of high-threshold Ca^{2+} channels with a high affinity for L-type channels in cerebellar granule neurons, Proc. Natl. Acad. Sci. U. S. A. 91 (1994) 878–882.
[53] J.K. Klint, G. Berecki, T. Durek, M. Mobli, O. Knapp, G.F. King, D.J. Adams, P.F. Alewood, L.D. Rash, Isolation, synthesis and characterization of ω-TRTX-Cc1a, a novel tarantula venom peptide that selectively targets L-type Ca_V channels, Biochem. Pharmacol. 89 (2014) 276–286.
[54] H. Kubista, R.A. Mafra, Y. Chong, G.M. Nicholson, P.S. Beirão, J.S. Cruz, S. Boehm, W. Nentwig, L. Kuhn-Nentwig, CSTX-1, a toxin from the venom of the hunting spider *Cupiennius salei*, is a selective blocker of L-type calcium channels in mammalian neurons, Neuropharmacology 2007 (1650-1662) 52.
[55] G.F. King, P. Escoubas, G.M. Nicholson, Peptide toxins that selectively target insect Na_V and Ca_V channels, Channels 2 (2008) 100–116.
[56] A. Touchard, A. Dejean, P. Escoubas, J. Orivel, Intraspecific variations in the venom peptidome of the ant *Odontomachus haematodus* (Formicidae: Ponerinae) from French Guiana, J. Hymenopt. Res. 47 (2015) 87.
[57] A. Touchard, Biodiversité, Biochimie et Pharmacologie Des Peptides De Venins De Fourmis(PhD Thesis) Université des Antilles et de la Guyane, Kourou, France, 2015.
[58] C. Schmidt, Molecular phylogenetics of ponerine ants (Hymenoptera: Formicidae: Ponerinae), Zootaxa 3647 (2013) 201–250.